THE JOURNAL OF BIOLOGICAL CHEMISTRY VOL. 290, NO. 6, pp. 3430–3439, February 6, 2015

Stanniocalcin-2 Inhibits Mammalian Growth by Proteolytic Inhibition of the Insulin-like Growth Factor Axis*

Received for publication, September 12, 2014, and in revised form, December 16, 2014 Published, JBC Papers in Press, December 22, 2014, DOI 10.1074/jbc.M114.611665

Malene R. Jepsen[1], Søren Kløverpris[1], Jakob H. Mikkelsen[1], Josefine H. Pedersen, Ernst-Martin Füchtbauer, Lisbeth S. Laursen, and Claus Oxvig[2]

From the Department of Molecular Biology and Genetics, Aarhus University, DK-8000 Aarhus, Denmark

Background: The biological function and biochemical activity of mammalian stanniocalcin-2 are unknown.
Results: Stanniocalcin-2 inhibits proteolytic release of insulin-like growth factor (IGF), and its ability to cause growth retardation upon transgenic overexpression in mice depends on its proteinase inhibitory function.
Conclusion: Stanniocalcin-2 is a novel component of the IGF axis.
Significance: Altered stanniocalcin-2 expression may affect IGF signaling under pathological conditions.

Mammalian stanniocalcin-2 (STC2) is a secreted polypeptide widely expressed in developing and adult tissues. However, although transgenic expression in mice is known to cause severe dwarfism, and targeted deletion of STC2 causes increased postnatal growth, its precise biological role is still unknown. We found that STC2 potently inhibits the proteolytic activity of the growth-promoting metalloproteinase, pregnancy-associated plasma protein-A (PAPP-A). Proteolytic inhibition requires covalent binding of STC2 to PAPP-A and is mediated by a disulfide bond, which involves Cys-120 of STC2. Binding of STC2 prevents PAPP-A cleavage of insulin-like growth factor-binding protein (IGFBP)-4 and hence release within tissues of bioactive IGF, required for normal growth. Concordantly, we show that STC2 efficiently inhibits PAPP-A-mediated IGF receptor signaling *in vitro* and that transgenic mice expressing a mutated variant of STC2, STC2(C120A), which is unable to inhibit PAPP-A, grow like wild-type mice. Our work identifies STC2 as a novel proteinase inhibitor and a previously unrecognized extracellular component of the IGF system.

The insulin-like growth factors (IGF-I and -II) are ubiquitous polypeptides, involved in cell proliferation and survival (1, 2). IGF signaling is mediated by the type 1 IGF receptor (IGF1R),[3] but six high affinity IGF-binding proteins, IGFBP-1 to 6, are able to sequester the IGFs from the receptor (3, 4). Compared with insulin signaling, the presence of IGFBPs thus represents an additional layer of regulation with differential synthesis of the different IGFBPs. However, bioactive IGF can be released by means of proteolytic cleavage of the binding protein, causing the generation of IGFBP fragments with diminished affinity for IGF (5). Specific and limited proteolysis represents the principal mechanism of IGF activation.

One IGF-releasing enzyme is the large metalloproteinase, pregnancy-associated plasma protein-A (PAPP-A, pappalysin-1, EC 3.4.24.79), a member of the metzincin superfamily of metalloproteinases (6), that is able to cleave IGFBP-4 (7), IGFBP-5 (8), and IGFBP-2 (9). PAPP-A functions intimately with IGFBP-4 (8, 10–15), and highly specific IGF-dependent (8) proteolytic cleavage by surface-tethered PAPP-A releases bioactive IGF from the inactive IGF·IGFBP-4 complex in close proximity to the receptor (16). In agreement with this mechanism, PAPP-A null mice (17) and IGF-II null mice (18) both have a 40% reduced body mass compared with wild-type littermates. PAPP-A is not only important in development, it is also thought to be involved in vascular disease in humans (19), and PAPP-A knock-out mice show resistance to the development of atherosclerotic lesions (20), diabetic nephropathy (21), and cancer (22). Similar to several other genes of the IGF axis, the absence of PAPP-A causes a markedly (35%) increased healthy life span in mice (23).

The stanniocalcins (STC1 and STC2) are widely expressed secreted glycoproteins. Numerous published studies have indicated the possible involvement of the two mammalian STCs in diverse biological processes such as cell proliferation, calcium regulation, and cancer development (24–26). However, their precise biological role remains unknown. Of particular interest, mice overexpressing STC2 are reduced 45% in size (27), whereas STC2 knock-out mice are 15% larger than wild-type littermates (28). Therefore, although the STCs have never been connected with the IGF system, we reasoned that STC2 might influence IGF signaling. In one possible scenario, supported by the severe proportional dwarf phenotype observed upon either overexpression of STC2 or knock-out of PAPP-A, STC2 might negatively affect the strong growth-promoting activity of PAPP-A.

EXPERIMENTAL PROCEDURES

Plasmid Constructs and Mutagenesis—A plasmid containing the coding sequence of human STC2 (nt. 1131–2216 of NM_003714.2 flanked by a 5′ XhoI site and a 3′ HindIII site) was purchased (Invitrogen). The cDNA was cloned into the XhoI/HindIII sites of pcDNA3.1/Myc-His(−)A (Invitrogen) to obtain pSTC2. Plasmid constructs encoding human PAPP-A

* This work was supported by grants from the Lundbeck Foundation, the Novo Nordisk Foundation, the Danish Council for Independent Research (Medical Sciences), and the Danish Genetically Modified Animal Resource.
[1] These authors contributed equally to this work.
[2] To whom correspondence should be addressed. E-mail: co@mbg.au.dk.
[3] The abbreviations used are: IGF1R, type 1 IGF receptor; IGFBP, IGF-binding protein; PAPP-A, pregnancy-associated plasma protein-A; STC, stanniocalcin; MEF, mouse embryonic fibroblast; nt., nucleotide.

(29), murine PAPP-A (30), and human IGFBP-4 (10) were reported elsewhere.

Mutagenesis of pSTC2 was carried out by QuikChange (Stratagene) using pSTC2 as a template, and the following sets of primers (numbering of NM_003714.2, mutated nucleotides underlined): 5′-GCACAGGTTCGGCGCCATAAGCCGGAAGTG-3′ (nt. 1655–1684) and 5′-CACTTCCGGCTTATGGCGCCGAACCTGTGC-3′ (nt. 1684–1655) for pSTC2(C120A); 5′-CAGCGTGCAGGTTCAGGCTGAGCAGAACTGGGGAAG-3′ (nt. 1883–1918) and 5′-CTTCCCCAGTTCTGCTCAGCCTGAACCTGCACGCTG-3′ (nt. 1918–1883) for pSTC2(C197A); and 5′-GAACTGGGGAAGCCTGGCCTCCATCTTGAGCTTC-3′ (nt. 1907–1940) and 5′-GAAGCTCAAGATGGAGGCCAGGCTTCCCCAGTTC-3′ (nt. 1940-1907) for pSTC2(C205A). The mutated cDNAs were swapped into pSTC2 using the XhoI/HindIII sites. All constructs were verified by sequence analysis.

Animal Experiments—For the production of transgenic mice, PCR fragments encoding untagged STC2 or STC2-(C120A) were generated by using the primers 5′-CGCAAATGGGCGGTAGGCGTG-3′ (nt. 769–789 of pcDNA3.1-Myc-His(−)A) and 5′-AAAAAAAGATCTTCACCTCCGGATATCAGAATACTC-3′ (nt. 2219–2196 of NM_003714.2, BglII site underlined), and pSTC2 and pSTC2(C120A), respectively, as templates. The PCR fragments were cloned into the XhoI/BglII sites of pCAGGS (BCCM, LMBP 2453 (31)) to generate pCAGGS-STC2 and pCAGGS-STC2(C120A). Plasmid DNA was linearized with PvuI and microinjected into male pronuclei of B6D2F2 zygotes (Taconic Farms), which were then introduced into pseudopregnant NMRI female mice (Taconic Farms). Transgenic mice, B6D2F2-Tg(STC2) or B6D2F2-Tg-(STC2(C120A)), were identified by PCR using primers specific for the pCAGGS plasmid (5′-AGGGCGCAGGGACTTCCTTTGTCCCAAATC-3′ (nt. 4448-4477 of pCAGGS)) and the cDNA (5′-TTCAAACACGCCACACCCCACATCGCCAG-3′ (nt. 1517–1489 of NM_003714.2)), and genomic DNA purified from tail biopsies. Of 44 mice resulting from pCAGGS-STC2-injections, nine were positive for the transgenic insert. Four of these gave rise to transgenic offspring with detectable levels of STC2 antigen in the serum, and they were used as founders for further breeding. Similarly, of 39 mice resulting from pCAGGS-STC2(C120A) injections, 11 were positive. Five of these gave rise to transgenic offspring with detectable levels of STC2 antigen in the serum and were used as founders. Founders were bred with C57BL/6JBomTac (Taconic Farms), giving rise to litters containing B6;D2-Tg(STC2)N1 or B6;D2-Tg(STC2-(C120A))N1 mice as well as wild-type littermates, which were genotyped and analyzed blinded for growth by consecutive weighing. At weeks 5 and 8, blood was drawn from the sublingual vein; serum was allowed to form, and the samples were frozen and stored at −20 °C until further analysis. For weight comparisons, mice were grouped according to individual serum levels of STC2. The mice were kept on a 12-h light/12-h dark cycle and given Altromin 1319 (Brogaarden) *ad libitum*. All mouse work was conducted with permission of the national Danish authorities (Dyreforsøgstilsynet).

Culture and Analysis of Mouse Embryonic Fibroblasts—Primary cultures of mouse embryonic fibroblasts (MEFs) were derived from E13.5 embryos resulting from mating B6;D2-Tg(STC2)N1 female and male littermates. The embryos were washed, minced, and digested with papain, and cell suspensions were plated in DMEM culture medium supplemented with 55 μM β-mercaptoethanol (Invitrogen). Cells at passages 2–4 were used for experiments. Residual tissue from each embryo was used for genotyping, and the presence of transgene-derived STC2 secreted into the culture media was confirmed by ELISA. Culture media from nontransgenic or transgenic MEFs were assessed for the presence of proteolytic activity toward IGFBP-4, with or without the addition of inhibitory mAb 1/41 (100 nM) (32).

Transgenic STC2 contained in the media of confluent plates was immunoprecipitated from 20 ml of media using 30 μl of protein G-Sepharose 4 Fast Flow (GE Healthcare), to which mAb STC221 was immobilized at 2 mg/ml by using dimethyl pimelimidate dihydrochloride (Sigma) cross-linking, essentially as described (33). Eluted protein was assessed for the presence of endogenous murine PAPP-A by Western blotting using mAb D8-mIgG2a.

Proteinase Assays—Purified IGFBP-4 was labeled with ^{125}I (Amersham Biosciences), and cleavage reactions were carried out as described previously (10, 34). In brief, media harvested from cells transfected with human PAPP-A cDNA with or without pSTC2 or pSTC2(C120A) were diluted (1:500) to 50 pM PAPP-A and mixed with preincubated ^{125}I-IGFBP-4 (10 nM) and IGF-II (100 nM) (GroPep Bioreagents) in 50 mM Tris-HCl, 100 mM NaCl, 1 mM $CaCl_2$, pH 7.5. Following 10–40 min of incubation at 37 °C, the reactions were terminated by the addition of hot SDS-PAGE sample buffer supplemented with 25 mM EDTA. Substrate and cleavage products were separated by 12% nonreducing SDS-PAGE and visualized by autoradiography using a storage phosphor screen (GE Healthcare) and a Typhoon imaging system (GE Healthcare). For some reactions, media from cells transfected with human or murine PAPP-A cDNA were incubated for 0 or 16 h at 37 °C with culture media containing a molar excess of STC2 prior to dilution and analysis of activity.

Cell Culture and Transfection—Human embryonic kidney 293T cells (293tsA1609neo) were maintained in high glucose DMEM supplemented with 10% fetal bovine serum, 2 mM glutamine, nonessential amino acids, and gentamicin (Invitrogen). For transient transfection, 6.0×10^6 cells were plated onto 10-cm dishes and transfected 18 h later by calcium phosphate coprecipitation using 10 μg of plasmid DNA prepared by GenElute HP plasmid miniprep kit (Sigma). Culture supernatants were harvested 48 h post-transfection and cleared by centrifugation, or the cells were further cultured in serum-free medium (CD293, Invitrogen) to facilitate purification. Secreted levels of PAPP-A were determined by a commercial ELISA (AL-101, Ansh Labs).

Protein Purification—Purification of His-tagged recombinant proteins was carried out by affinity chromatography on a 1-ml HisTrap HP column (GE Healthcare). Serum-free media were diluted 1:1 in 20 mM NaH_2PO_4, 150 mM NaCl, pH 7.4 (PBS), and loaded onto the column with a flow rate of 1 ml/min. The column was washed with 20 column volumes of 50 mM NaH_2PO_4, 1 M NaCl, 20 mM imidazole, 0.05% Tween 20, pH 7.4,

followed by 5 column volumes of PBS. The proteins were eluted with 50 mM NaH_2PO_4, 300 mM imidazole, pH 7.4, and dialyzed against 20 mM HEPES, 150 mM NaCl, pH 7.4. Prior to iodination, IGFBP-4 was further purified by reversed-phase (RP)-HPLC on a Discovery BIO wide pore C5 column (4 × 250 mm, Sigma), as described (16). Protein purity was assessed by SDS-PAGE, and quantification of purified proteins was done by amino acid analysis.

Primary Antibodies—For Western blotting, the following antibodies were used: rabbit polyclonal anti-(human PAPP-A) (35); mouse monoclonal anti-(c-Myc) (9E10, ATCC); goat polyclonal anti-(human STC2) (R&D Systems, AF2830); mouse monoclonal PY99 (Santa Cruz Biotechnology, sc-7020) for detection of phosphotyrosine residues; mouse monoclonal CT-1 (GroPep Bioreagents, MAJ1) for detection of human IGF receptor (IGF1R); mouse monoclonal AC-74 (Sigma, A5316) for detection of β-actin, and mouse monoclonal D8-mIgG2a (36) for detection of murine PAPP-A. For use in ELISA and for immunoprecipitation, monoclonal antibodies (STC216, STC220, STC221, STC225, STC239, and STC243) against human STC2[4] were used. For biotinylation, mAb STC216 was incubated at 7.4 μM with a 20-fold molar excess of EZ-Link Sulfo-NHS-LC-Biotin (Thermo Fisher Scientific, catalog no. 21335) on ice for 2 h. The reaction was stopped with 10 mM Tris-HCl and dialyzed against 20 mM HEPES, 150 mM NaCl, pH 7.5.

Enzyme-linked Immunosorbent Assays (ELISA)—For measurement of STC2 concentration, 96-well plates (MaxiSorp, Nunc) were coated with 100 μl per well of 7.5 μg/ml of catching antibody (mAb STC221) in 100 mM Na_2HCO_3, pH 9.4, by overnight incubation at 4 °C. The wells were then blocked with 200 μl per well of 2% bovine serum albumin (BSA) in TBS (30 mM Tris-HCl, 300 mM NaCl, 2 mM $CaCl_2$, pH 7.4) for 30 min at 37 °C. Samples were diluted in TBS-T (TBS containing 0.05% Tween 20) supplemented with 1% BSA and incubated in the coated wells for 1 h at 37 °C. Following washing in TBS-T, the wells were incubated for 1 h at 37 °C with biotinylated detecting antibody (STC216) diluted in TBS-T with 1% BSA to 1 μg/ml, washed again, and incubated (1 h) with avidin-conjugated horseradish peroxidase (P0347, DAKO) diluted 1:20,000 in TBS-T with 1% BSA. Following a final round of washing, the wells were developed using OPD tablets (S2045, DAKO). Calibrators were based on recombinant STC2 diluted in TBS-T with 1% BSA. Eight calibration points (6.25–800 ng/ml) were used. Absorbance was measured at 490 nm on an EnSpire Multimode Plate Reader (PerkinElmer Life Sciences). Blank values were subtracted, and data were analyzed by using cubic curve fitting. The functional sensitivity of the assay at 20% coefficient of variation was 20 ng/ml.

To assess monoclonal antibody binding to STC2 and STC2(C120A), plates were coated with 100 μl per well of 2 μg/ml polyclonal anti-(STC2). Detection was carried out with available STC2 mAbs (1 μg/ml) followed by anti-mouse IgG-HRP (DAKO, P0260) diluted 1:2000. Signals from dilution series of STC2 and STC2(C120A) were normalized and compared for each of the antibodies. Buffers for dilution and washing were as described above.

Immunoblotting and Analysis of Complex Formation—Proteins separated by reducing or nonreducing SDS-PAGE were blotted onto a PVDF membrane (Millipore), blocked with 2% Tween 20, and equilibrated in 50 mM Tris-HCl, 500 mM NaCl, 0.1% Tween 20, pH 9.0 (TST). Primary antibodies were diluted (to 1–5 μg/ml) in TST containing 0.5% fetal bovine serum, and blots were incubated overnight at room temperature. The blots were incubated for 1 h at room temperature with secondary antibodies (polyclonal swine anti-rabbit IgG-HRP (DAKO, P0217), polyclonal rabbit anti-goat IgG-HRP (DAKO, P0160), or polyclonal rabbit anti-mouse IgG-HRP (DAKO, P0260)) diluted 1:2000 in TST containing 0.5% fetal bovine serum. All washing between the steps was carried out with TST. The blots were developed using enhanced chemiluminescence (ECL Prime, GE Healthcare), and images were captured and analyzed using an ImageQuant LAS 4000 instrument (GE Healthcare). All gel images and immunoblots shown are representative of at least four independent experiments.

To probe for covalent complex formation between proteins synthesized in separate cells, culture media were incubated 0–16 h at 37 °C, separated by nonreducing SDS-PAGE (2 μl per lane), and then analyzed by Western blotting as described above. Media from cotransfected cells were not incubated prior to analysis.

Circular Dichroism (CD) Analysis—Purified wild-type and mutant proteins were compared by using circular dichroism analysis (37). Prior to analysis, purified proteins were dialyzed against 20 mM NaH_2PO_4, 20 mM NaF, pH 7.4. Ten CD spectra were recorded at 25 °C for each protein on a Jasco J-810 spectropolarimeter (Jasco Spectroscopic, Japan) using a polypeptide concentration of 0.5 mg/ml and a cuvette of 2 mm path length. CD data were obtained in the range from 260 to 190 nm at a resolution of 0.2 nm using a bandwidth of 1.0 nm. The scan speed was 100 nm/min, and the response time was 1 s. Temperature scans were carried out in the range from 260 to 200 nm. $\Delta\epsilon$ (expressed in degrees × cm^2/dmol) values were calculated on the basis of a mean molar mass of 110 g/mol/residue.

IGF1R Stimulation Assay—A cell line stably expressing IGF1R, 293-IGFR (clone H), was used to measure IGF receptor phosphorylation, essentially as described (16). Starved cells were rinsed in PBS containing $CaCl_2$ (0.1 mg/liter) and $MgCl_2$ (0.1 mg/liter), pH 7.4, and stimulated for 15 min with combinations of IGF-I (10 nM), IGFBP-4 (50 nM), PAPP-A (2.5 nM), and STC2 (15 nM). Before stimulation, IGF-I and IGFBP-4 were incubated for 20 min at 37 °C in 20 mM HEPES, 100 mM NaCl, 1 mM $CaCl_2$, pH 7.5, to allow the IGF-I·IGFBP-4 complex to form. PAPP-A was then added, and cleavage reactions were carried out in the same buffer for 20 min at 37 °C. Prior to use, PAPP-A was incubated with or without STC2 or STC2(C120A) in serum medium for 16 h at 37 °C. The stimulated cells were lysed on ice with RIPA buffer (Sigma, R0278) and supplemented with proteinase inhibitor mixture (Sigma, P8340) and phosphatase inhibitor mixture set II (EMD Millipore, 524625) for 10 min. Western blotting of cleared and reduced lysates was used to quantitate β-subunit phosphorylation using mAb PY99. Detection of total IGF receptor was done using mAb CT-1. For loading controls, blots were stripped and reprobed with actin mAb AC-74. Quantifica-

[4] S. Mistry, A. Kumar, and C. Oxvig, unpublished data.

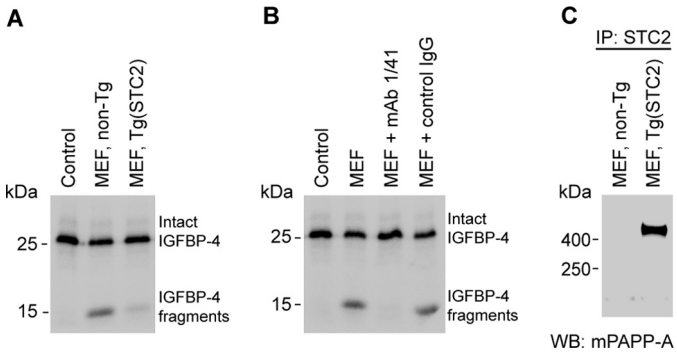

FIGURE 1. **Analysis of cultured MEFs derived from STC2 transgenic mice and nontransgenic littermates.** *A,* proteolytic activity toward radiolabeled IGFBP-4 in medium conditioned by MEFs derived from STC2 transgenic mice or nontransgenic littermates (E13.5). Note that MEFs from Tg(STC2) mice contain only residual proteolytic activity. *B,* proteolytic activity toward radiolabeled IGFBP-4 in MEF medium derived from nontransgenic mice in the presence or absence of mAb 1/41 (32), a specific inhibitor of PAPP-A. *C,* co-immunoprecipitation (*IP*) of transgenic STC2 and endogenous PAPP-A from MEF medium derived from STC2 transgenic mice. Separation was done by nonreducing SDS-PAGE. *WB,* Western blot.

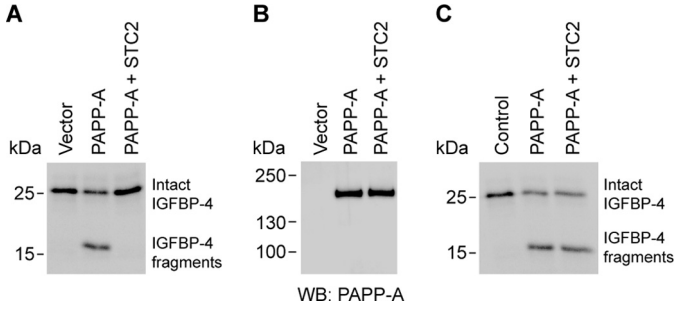

FIGURE 2. **PAPP-A activity is eliminated by cotransfection with STC2 cDNA but not by the addition of purified STC2 protein.** *A,* PAPP-A proteolytic activity toward radiolabeled IGFBP-4 in media from HEK293T cells transfected with combinations of cDNAs as indicated. Cotransfection with STC2 cDNA appears to inhibit PAPP-A activity. *B,* PAPP-A Western blot (*WB*) of samples from *A* demonstrating similar levels of PAPP-A secretion from the transfected cells. Separation was done by reducing SDS-PAGE. *C,* PAPP-A proteolytic activity toward radiolabeled IGFBP-4 in the presence or absence of purified STC2 added at the beginning of the cleavage reaction. Note that in this experiment, STC2 did not inhibit PAPP-A.

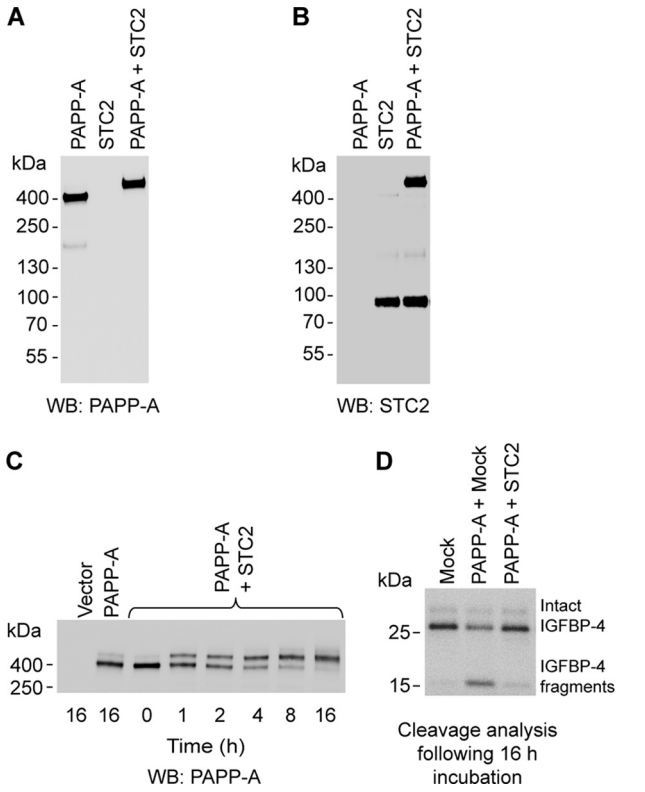

FIGURE 3. **Inhibition of PAPP-A proteolytic activity by STC2 requires covalent complex formation.** *A,* PAPP-A Western blot (*WB*) of medium from HEK293T cells transfected with combinations of cDNAs as indicated. Note the change in migration of PAPP-A upon cotransfection with STC2 cDNA. *B,* STC2 Western blot of samples from *A*. Note the appearance of a high molecular weight band upon cotransfection with PAPP-A cDNA. *C,* PAPP-A Western blot of separately synthesized PAPP-A and STC2 incubated for 0–16 h. SDS-PAGE separations for *A–C* were done under nonreducing conditions. *D,* PAPP-A proteolytic activity toward radiolabeled IGFBP-4 in 16-h samples from *C*.

tion of band intensities was carried out using an ImageQuant LAS 4000 instrument (GE Healthcare). The signals of mAb PY99 were subtracted background signals and plotted.

Statistical Analysis—All statistical analyses were performed using GraphPad Prism version 5.0. Statistical analyses of mouse postnatal growth data were performed using the unpaired Student's *t* test for each time point. Statistical analysis of IGF-I receptor signaling was performed using one-way analysis of variance followed by Dunnett's test. Statistical analysis of antibody binding was performed using one-way analysis of variance followed by Tukey's test. $p < 0.05$ was considered statistically significant.

RESULTS

Culture Medium of Embryonic Fibroblasts Derived from STC2 Transgenic Mice Shows a Marked Reduction in Proteolytic Activity toward IGFBP-4—To test the hypothesis that PAPP-A and STC2 represent an antagonistic pair whose balance may be important for the regulation of IGF signaling, we first generated mice transgenic for human STC2. We find that medium conditioned by MEFs derived from nontransgenic littermates showed specific cleavage of IGFBP-4, whereas medium conditioned by MEFs from STC2 transgenic mice showed a marked reduction in proteolytic activity toward IGFBP-4 (Fig. 1*A*). We further find that the proteolytic activity toward IGFBP-4, present in medium conditioned by MEFs from nontransgenic mice, can be completely inhibited by using a novel inhibitory monoclonal antibody specific for PAPP-A (Fig. 1*B*) (32). The latter experiment demonstrates that the IGFBP-4 proteolytic activity secreted by MEFs can be attributed to PAPP-A, and it is in agreement with the earlier finding that MEFs derived from PAPP-A knock-out mice lack proteolytic activity toward IGFBP-4 (17). Together these experiments indicate that either PAPP-A synthesis, secretion, or activity is compromised upon transgenic expression of STC2.

STC2 Present in Culture Medium of Embryonic Fibroblasts Derived from STC2 Transgenic Mice Is Associated with PAPP-A—To probe for a possible association between STC2 and PAPP-A, coimmunoprecipitation was attempted using an STC2-specific antibody followed by PAPP-A Western blotting. In MEF medium from STC2 transgenic mice, but not from nontransgenic littermates, a single band of high molecular weight, which contained strong PAPP-A immunoreactivity, was observed (Fig. 1*C*). This experiment allows us to conclude that a physical interaction between the trans-

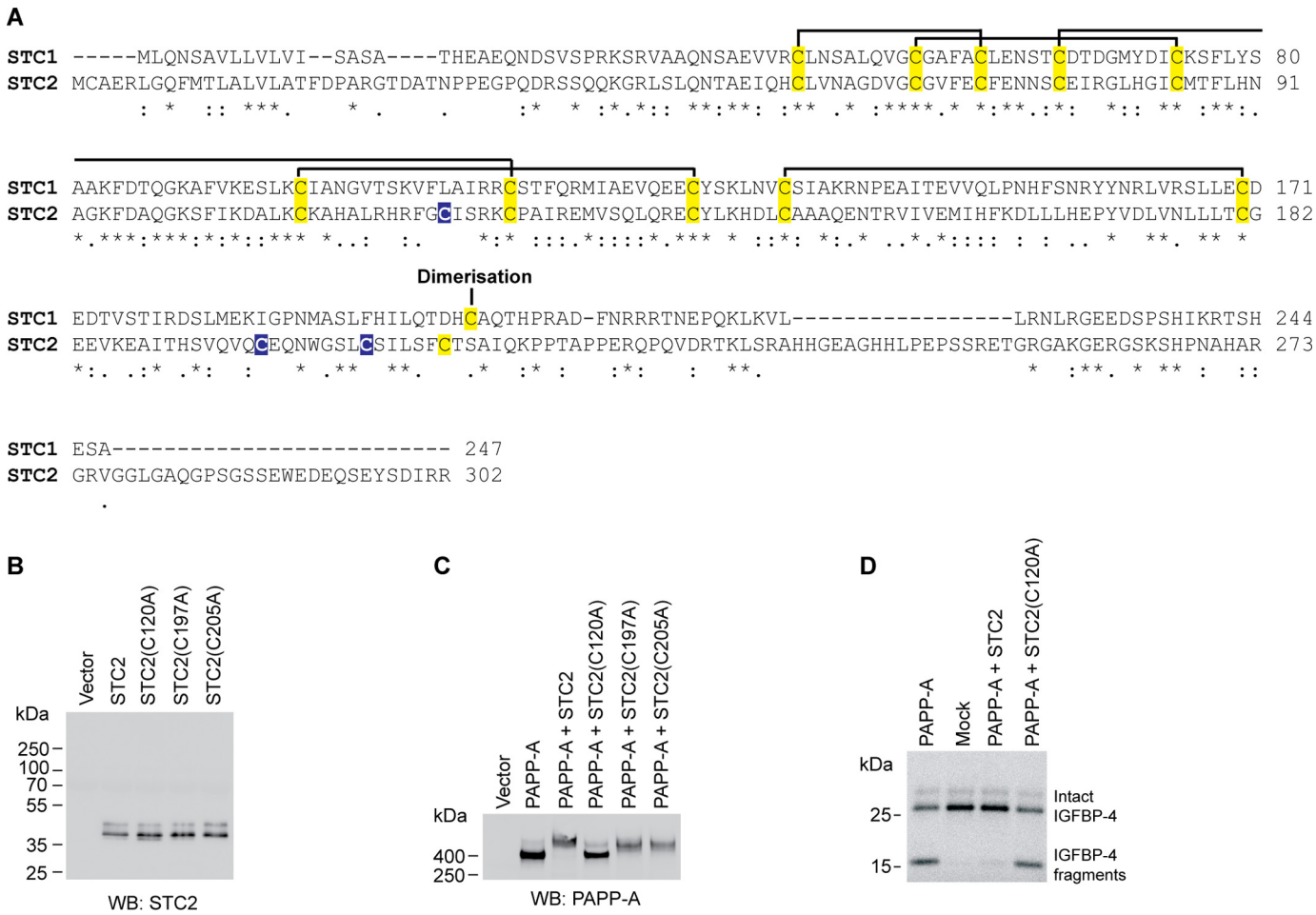

FIGURE 4. **Cys-120 of STC2 is required for covalent complex formation and proteolytic inhibition.** *A,* sequence alignment of human STC1 (NM_003155.2) and STC2 (NM_003714.2) using Clustal Omega. Disulfide bonds and dimerization disulfide of STC1, indicated by *lines*, are according to published data (38). Three cysteine residues of STC2 (Cys-120, Cys-197, and Cys-205), which have no counterpart in STC1, are indicated in *blue*. Cys-120 is conserved in all known mammalian STC2 sequences, and it has no counterpart in any known STC1 sequence (data not shown). *B,* STC2 Western blot following reducing SDS-PAGE of medium from HEK293T cells transfected with wild-type or mutated variants of STC2 cDNA as indicated. *C,* PAPP-A Western blot (*WB*) following nonreducing SDS-PAGE of media from HEK293T cells transfected with combinations of cDNAs as indicated. Note that STC2(C120A) is unable to form a covalent complex with PAPP-A. *D,* proteolytic activity toward radiolabeled IGFBP-4 in medium from HEK293T cells transfected with cDNA encoding PAPP-A, preincubated for 16 h with or without STC2 or STC2(C120A).

genic STC2 and the endogenous PAPP-A occurs in the MEF medium, suggesting that STC2 might act to inhibit PAPP-A proteolytic activity.

STC2 Forms a Covalent Complex with PAPP-A and Irreversibly Inhibits Its Proteolytic Activity—We further analyzed the interaction between STC2 and PAPP-A *in vitro* in a system based on human recombinant proteins. PAPP-A secreted from transfected mammalian cells rapidly cleaves IGFBP-4 at a single site, resulting in two proteolytic fragments that comigrate in SDS-PAGE (34). However, no proteolytic activity toward IGFBP-4 was detected upon cotransfection with STC2 cDNA (Fig. 2*A*), even though PAPP-A was still secreted from the cells (Fig. 2*B*). Therefore, to directly test the hypothesis that STC2 is an inhibitor of PAPP-A, separately synthesized and purified STC2 was added to the cleavage reaction. Surprisingly, STC2 did not cause an alteration of PAPP-A activity in this experiment (Fig. 2*C*).

Following separate transfection, PAPP-A and STC2 migrated in SDS-PAGE as dimers with the expected sizes of ~400 and 90 kDa, respectively, but upon cotransfection, a high molecular mass band of ~500 kDa, which contained both antigens, was formed (Fig. 3, *A* and *B*). Thus, STC2 is capable of forming a complex with PAPP-A, which resists separation in denaturing PAGE and therefore most likely is covalent. However, from this experiment, we cannot distinguish between complex formation before or after protein secretion.

We further analyzed the process of PAPP-A·STC2 complex formation by incubating separately synthesized PAPP-A and STC2. A PAPP-A-containing band of 500 kDa gradually appeared during the incubation (Fig. 3*C*), demonstrating that complex formation in the extracellular environment is possible. PAPP-A was proteolytically active following incubation in the absence of STC2, while after 16 h of incubation with STC2, PAPP-A showed no activity (Fig. 3*D*). Importantly, this explains the lack of STC2 inhibitory activity observed without prolonged preincubation (Fig. 2*C*).

Based on the above, we conclude that STC2 is a potent proteinase inhibitor of PAPP-A. Curiously, inhibition requires formation of a covalent complex between PAPP-A and STC2. For-

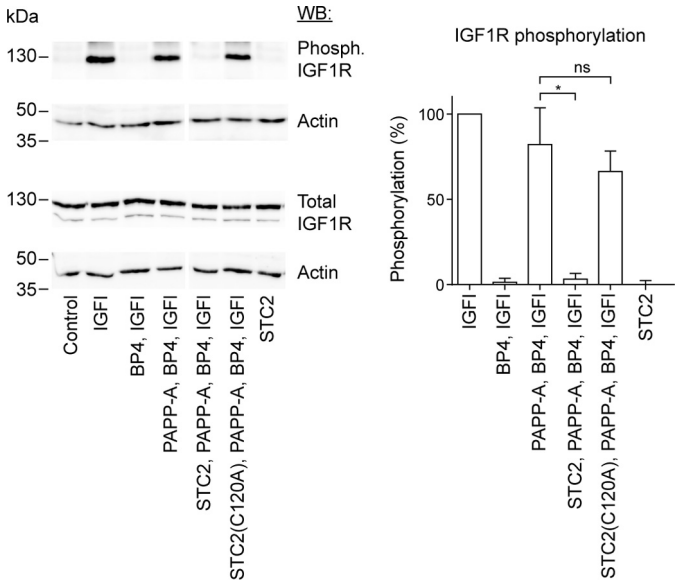

FIGURE 5. **STC2, but not STC2(C120A), abrogates PAPP-A-mediated IGF1R signaling *in vitro*.** Cells expressing IGF1R were stimulated with combinations of IGF-I, IGFBP-4, PAPP-A, and STC2/STC2(C120A) as indicated, and cell lysates were analyzed by Western blotting (*WB*). Quantified signals of IGF receptor phosphorylation normalized to the signal with IGF-I alone are shown to the *right*. Results are means ± S.D. from four independent experiments (*ns*, not statistically significant; *, $p < 0.0001$).

mation of this complex appears to be a relatively slow process under the given experimental conditions.

Abilities of STC2 to Covalently Bind and Inhibit PAPP-A and to Inhibit IGF Signaling in Vitro Depend on Cys-120—The homologous STC1 contains 11 cysteine residues. It has previously been shown that 10 of these form five intramolecular disulfide bonds, and that one residue is responsible for dimerization (38). These 11 cysteine residues are conserved in STC2, which contains three additional cysteines, Cys-120, Cys-197, and Cys-205 (Fig. 4*A*). This uneven number of additional cysteines prompted us to test the possibility that formation of the PAPP-A·STC2 complex might be based on disulfide bonding between PAPP-A and STC2.

When the three additional cysteine residues were substituted individually to alanine, the level of protein expression was unchanged (Fig. 4*B*). However, one mutant, STC2(C120A), did not form a covalent complex with PAPP-A (Fig. 4*C*), indicating that an intermolecular disulfide bond involving Cys-120 is the basis for the covalent linkage between STC2 and PAPP-A. Furthermore, STC2(C120A) lacked the ability to inhibit PAPP-A under conditions where PAPP-A activity was eliminated by wild-type STC2 (Fig. 4*D*).

We then used a cell-based assay to assess the ability of STC2 to inhibit IGF receptor signaling *in vitro*. We find that STC2 virtually eliminated PAPP-A-mediated IGF receptor phosphorylation, whereas the effect of STC2(C120A) was nonsignificant (Fig. 5). Thus, not only the ability of STC2 to covalently bind PAPP-A but also its ability to inhibit PAPP-A-mediated IGF signaling is effectively disabled upon mutation of Cys-120.

STC2 Causes Growth Retardation in Mice by Proteolytic Inhibition—Prior to use for *in vivo* studies, we compared wild-type STC2 and STC2(C120A) to verify that the single amino acid substitution of residue Cys-120 did not impose a change in properties of the protein, except for the lost ability of STC2(C120A) to inhibit PAPP-A. Comparison by CD analysis showed similar spectra (Fig. 6*A*) of the purified proteins, and furthermore, the CD spectra of both STC2 and STC2(C120A) appeared to be unaffected by a transient exposure to 90 °C (Fig. 6*B*). These data suggest that the structural integrity of STC2(C120A) is intact. In addition, equal recognition of STC2 and STC2(C120A) by six available monoclonal antibodies also supported this interpretation (Fig. 6*C*). Finally, we verified that the biochemical properties of both STC2 and STC2(C120A) are conserved in the murine system (Fig. 6, *D* and *E*).

To finally test the hypothesis that overexpression of STC2 causes growth retardation by proteolytic inhibition, we generated mice transgenic for wild-type STC2 or STC2(C120A) in parallel. In agreement with earlier findings (27), overexpression of wild-type STC2 caused a severe reduction in postnatal growth rate compared with nontransgenic animals (Fig. 7*A*). Our data further indicate a correlation between the circulating level of STC2 and the severity of the growth retardation (Fig. 7*B*). In striking contrast, transgenic expression of STC2-(C120A) did not cause a detectable alteration in growth rate, even at high levels of circulating protein (Fig. 7*C*). We therefore draw the conclusion that STC2 transgenic mice show growth retardation because the proteolytic activity of PAPP-A is compromised.

DISCUSSION

We have identified STC2 as a potent inhibitor of PAPP-A proteolytic activity. STC2 binds covalently to PAPP-A to completely eliminate its activity toward IGFBP-4 and hence PAPP-A-mediated IGF signaling. From previous studies, it is known that although both transgenic overexpression of STC2 (27) and knock-out of PAPP-A (17) cause severe growth retardation, STC2 knock-out mice (28) are larger than wild-type mice. We here further show that mice transgenic for STC2(C120A), which is unable to inhibit PAPP-A, show normal growth (Fig. 8*A*).

The substantially increased body weight of STC2 knock-out mice (28) suggests that the absence of STC2 causes an elevated PAPP-A activity. A strong anabolic effect of PAPP-A was also demonstrated by a markedly increased bone thickness upon targeted transgenic PAPP-A expression in osteoblasts (39) and similarly by a large increase in skeletal muscle mass upon muscle-specific transgenic expression of PAPP-A (40). Finally, in humans, the growth-promoting potential of PAPP-A is underscored by the finding of a strong, positive correlation between birth weight and maternal first trimester levels of PAPP-A (41).

Taken together, these findings support a model in which a local dynamic balance between PAPP-A proteolytic activity and STC2 inhibitory activity is a critical determinant of IGF receptor stimulation *in vivo* (Fig. 8*B*). In this regard, it is important to stress that IGF-mediated growth ultimately depends on the level of pericellular, bioactive IGF in the tissue microenvironment (2). The source of IGF within tissues may be the circulation or cells of the tissue, first emphasized by the finding that liver-specific knock-out of IGF-I dramatically reduces (by 75%) serum levels of IGF-I but has no effect on growth (42, 43). It is also emphasized by the observation that the level of circu-

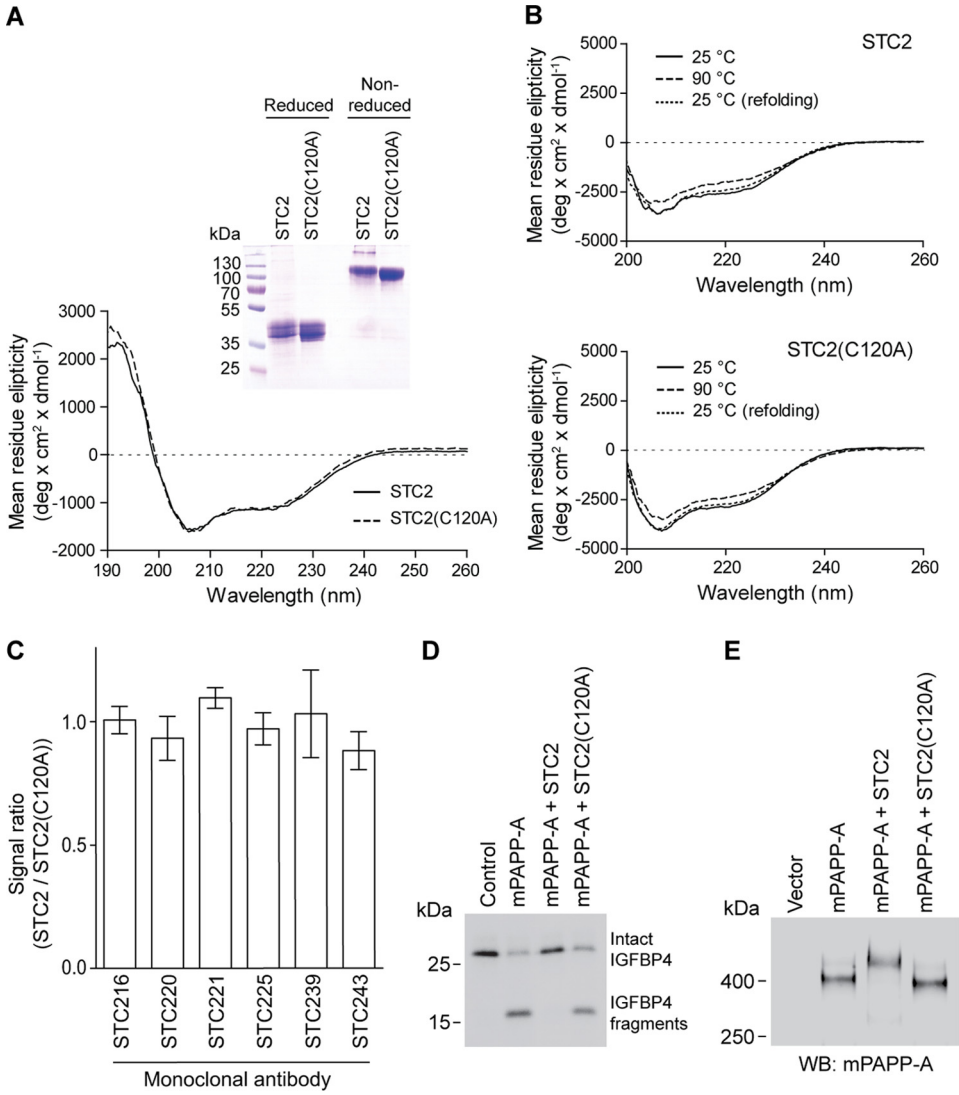

FIGURE 6. **Biochemical properties of STC2 are retained in STC2(C120A).** *A,* CD analysis of purified STC2 and STC2(C120A). *Inset* shows Coomassie-stained SDS-polyacrylamide gel of purified STC2 and STC2(C120A). *B,* CD spectra of STC2 and STC2(C120A) recorded at 25 and 90 °C and again at 25 °C following incubation at 90 °C for 2 min. *C,* relative binding of available monoclonal antibodies to STC2 and STC2(C120A) is plotted as a ratio between the levels measured in ELISAs. A value of 1 indicates equal binding to STC2 and STC2(C120A). Results are means ± S.D. from four independent experiments performed in triplicate. Differences in ratios are not statistically significant. *D,* proteolytic activity toward radiolabeled IGFBP-4 in medium from HEK293T cells transfected with cDNA encoding murine PAPP-A (mPAPP-A), preincubated with or without STC2 or STC2(C120A). *E,* Western blot (*WB*) following nonreducing SDS-PAGE of samples from *D* demonstrating covalent complex formation between murine PAPP-A and STC2 but not STC2(C120A).

lating IGF-I is not altered in mice that have become dwarfs as a result of STC2 overexpression (27).

In humans, adult height is influenced by genetic variants distributed in a large number of loci (44). Genes of these loci tend to group in known biological pathways, such as the IGF system, which was found to be represented by genes encoding IGF1R and PAPP-A, for example. Although not connected with any biological pathway, the gene encoding STC2 also appeared in this analysis. Similar findings have recently resulted from genetic studies of domestic dogs, which show the greatest variation in body size of any land mammal (45). It was found that the occurrence of derived variants at only six genes is a major explanation for the extreme reduction in body size of dogs caused by selective breeding (46). The authors found *STC2* to be among the genes, also including *IGF1* and *IGF1R*. Therefore, at least three of these six genes driving the small size of dogs are now connected with the IGF system.

Our finding that STC2 is a proteinase inhibitor is surprising. The two homologous STCs have unique amino acid sequences (47, 48), containing no known modules or motifs by which this biochemical function might have been predicted. Although the sequence of STC1 lacks a cysteine residue corresponding to Cys-120 of STC2, it is obvious to speculate that STC1 has biochemical properties similar to STC2. In this regard, it is interesting to note that transgenic overexpression of STC1 (49) also causes growth retardation, although STC1 knock-out mice are normal (50). STC1 may not be able to bind PAPP-A covalently, but a high affinity noncovalent interaction with PAPP-A might compensate for this. Future studies are required to address these questions. Likewise, further analysis is required to determine whether the STCs possess inhibitory activity toward other proteinases, including PAPP-A2 (51), the only paralog of PAPP-A. Because of the striking similarity in phenotypes between PAPP-A knock-out mice and transgenic STC2 mice, it

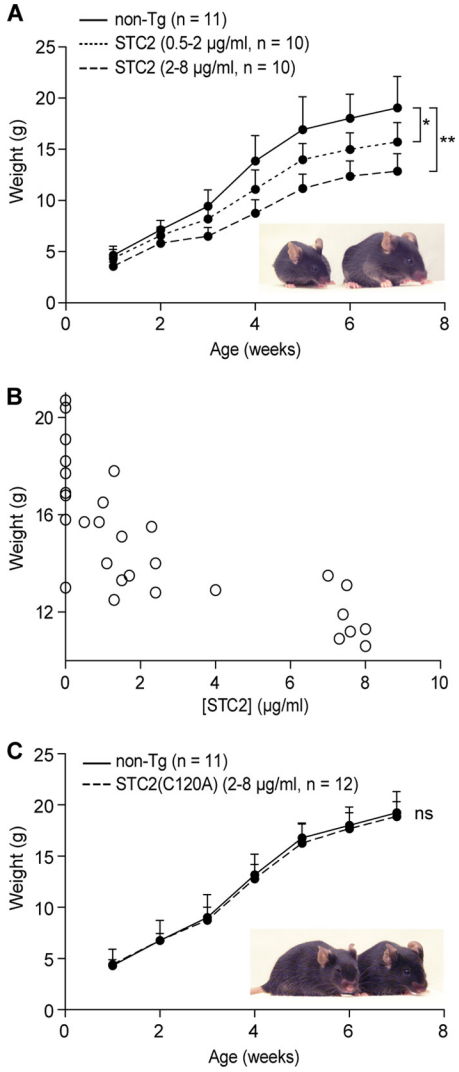

FIGURE 7. **Overexpression of STC2, but not STC2(C120A), causes growth retardation in mice.** *A,* growth curves of nontransgenic and STC2 transgenic female mice divided into groups according to circulating levels of STC2. Results are means with S.D. indicated. Statistical significance is based on comparison of mice older than 3 weeks (*, $p < 0.02$; **, $p < 0.0001$). The *inset* shows a transgenic mouse representative of the group with high (2–8 μg/ml) expression of STC2 (*left*) and a nontransgenic littermate. *B,* body weight of STC2 transgenic female mice at week 6 against measured levels of circulating transgene-derived STC2. *C,* growth curves of nontransgenic and STC2(C120A) transgenic female mice. The *inset* shows a transgenic mouse with high (2–8 μg/ml) expression of STC2(C120A) (*left*) and a nontransgenic littermate. Results are means with S.D. indicated. *ns*, not statistically significant.

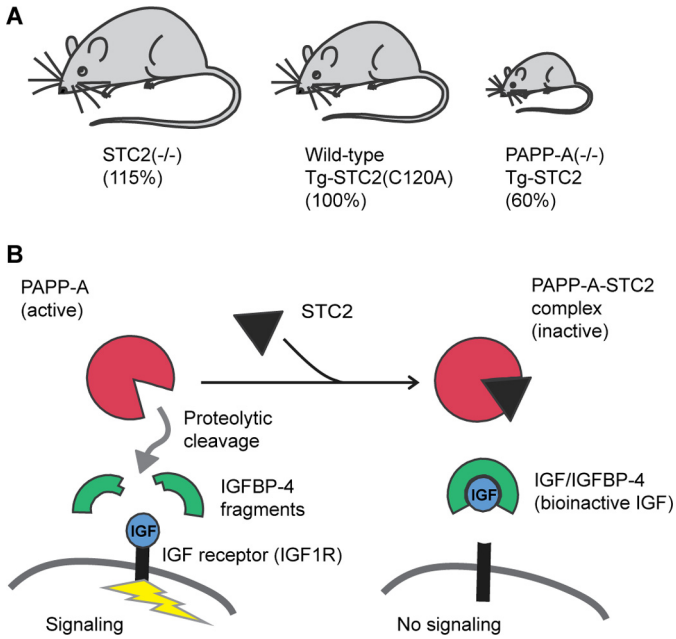

FIGURE 8. **STC2 and PAPP-A, consequences of genetic manipulation in mice and working model of their role in the IGF system.** *A,* size comparison of mice with targeted deletion of STC2 (28) or PAPP-A (17), or transgenic overexpression of STC2 (27) or STC2(C120A). *B,* model depicting the balance between active and STC2-inhibited PAPP-A, indirectly affecting IGF receptor (IGF1R) stimulation.

is tempting to speculate that the STCs do not affect proteinases other than PAPP-A. However, because knock-out of PAPP-A2 also causes a growth retardation phenotype in mice, albeit less severe than caused by knock-out of PAPP-A (52), PAPP-A2 might also be an STC target proteinase.

Dysregulated IGF receptor signaling has been extensively linked to various diseases, in particular human cancer (53). Also, the involvement of PAPP-A in cancer development is increasingly recognized (32), and is underscored by the finding that PAPP-A knock-out mice have a remarkably low incidence of spontaneous age-related tumors (22). It is therefore interesting that multiple reports link both stanniocalcins to human cancers, although both up- and down-regulations have been reported (24, 26). For example, loss of BRCA1 tumor suppressor function in breast cancer causes STC1 expression to become undetectable (54), and late relapse of breast cancer correlates with high expression of STC1 and STC2 (55).

Overall, we have demonstrated that STC2 is a novel proteinase inhibitor of PAPP-A, and therefore is most likely a part of the complex extracellular network that regulates IGF receptor activation *in vivo*. Our findings connect two areas of research that previously seemed unrelated. Future work will delineate the details of the concerted actions of these molecules in normal and pathological tissues.

Acknowledgments—We thank Sanne N. Andersen and Lisbeth A. Hansen for technical assistance, and Lars Sottrup-Jensen for help with circular dichroism analysis. We thank Søren K. Moestrup for helpful discussion.

REFERENCES

1. Stewart, C. E., and Rotwein, P. (1996) Growth, differentiation, and survival: multiple physiological functions for insulin-like growth factors. *Physiol. Rev.* **76,** 1005–1026
2. Ohlsson, C., Mohan, S., Sjögren, K., Tivesten, A., Isgaard, J., Isaksson, O., Jansson, J. O., and Svensson, J. (2009) The role of liver-derived insulin-like growth factor-I. *Endocr. Rev.* **30,** 494–535
3. Jones, J. I., and Clemmons, D. R. (1995) Insulin-like growth factors and their binding proteins: biological actions. *Endocr. Rev.* **16,** 3–34
4. Forbes, B. E., McCarthy, P., and Norton, R. S. (2012) Insulin-like growth factor binding proteins: a structural perspective. *Front. Endocrinol.* **3,** 38
5. Sitar, T., Popowicz, G. M., Siwanowicz, I., Huber, R., and Holak, T. A. (2006) Structural basis for the inhibition of insulin-like growth factors by insulin-like growth factor-binding proteins. *Proc. Natl. Acad. Sci. U.S.A.* **103,** 13028–13033
6. Cerdà-Costa, N., and Gomis-Rüth, F. X. (2014) Architecture and function of metallopeptidase catalytic domains. *Protein Sci.* **23,** 123–144
7. Lawrence, J. B., Oxvig, C., Overgaard, M. T., Sottrup-Jensen, L., Gleich,

G. J., Hays, L. G., Yates, J. R., 3rd, and Conover, C. A. (1999) The insulin-like growth factor (IGF)-dependent IGF binding protein-4 protease secreted by human fibroblasts is pregnancy-associated plasma protein-A. *Proc. Natl. Acad. Sci. U.S.A.* **96,** 3149–3153
8. Laursen, L. S., Overgaard, M. T., Søe, R., Boldt, H. B., Sottrup-Jensen, L., Giudice, L. C., Conover, C. A., and Oxvig, C. (2001) Pregnancy-associated plasma protein-A (PAPP-A) cleaves insulin-like growth factor binding protein (IGFBP)-5 independent of IGF: implications for the mechanism of IGFBP-4 proteolysis by PAPP-A. *FEBS Lett.* **504,** 36–40
9. Gérard, N., Delpuech, T., Oxvig, C., Overgaard, M. T., and Monget, P. (2004) Proteolytic degradation of IGF-binding protein (IGFBP)-2 in equine ovarian follicles: involvement of pregnancy-associated plasma protein-A (PAPP-A) and association with dominant but not subordinated follicles. *J. Endocrinol.* **182,** 457–466
10. Boldt, H. B., Overgaard, M. T., Laursen, L. S., Weyer, K., Sottrup-Jensen, L., and Oxvig, C. (2001) Mutational analysis of the proteolytic domain of pregnancy-associated plasma protein-A (PAPP-A): classification as a metzincin. *Biochem. J.* **358,** 359–367
11. Laursen, L. S., Overgaard, M. T., Nielsen, C. G., Boldt, H. B., Hopmann, K. H., Conover, C. A., Sottrup-Jensen, L., Giudice, L. C., and Oxvig, C. (2002) Substrate specificity of the metalloproteinase pregnancy-associated plasma protein-A (PAPP-A) assessed by mutagenesis and analysis of synthetic peptides: substrate residues distant from the scissile bond are critical for proteolysis. *Biochem. J.* **367,** 31–40
12. Boldt, H. B., Kjaer-Sorensen, K., Overgaard, M. T., Weyer, K., Poulsen, C. B., Sottrup-Jensen, L., Conover, C. A., Giudice, L. C., and Oxvig, C. (2004) The Lin12-notch repeats of pregnancy-associated plasma protein-A bind calcium and determine its proteolytic specificity. *J. Biol. Chem.* **279,** 38525–38531
13. Bale, L. K., and Conover, C. A. (2005) Disruption of insulin-like growth factor-II imprinting during embryonic development rescues the dwarf phenotype of mice null for pregnancy-associated plasma protein-A. *J. Endocrinol.* **186,** 325–331
14. Weyer, K., Boldt, H. B., Poulsen, C. B., Kjaer-Sorensen, K., Gyrup, C., and Oxvig, C. (2007) A substrate specificity-determining unit of three Lin12-Notch repeat modules is formed in trans within the pappalysin-1 dimer and requires a sequence stretch C-terminal to the third module. *J. Biol. Chem.* **282,** 10988–10999
15. Ning, Y., Schuller, A. G., Conover, C. A., and Pintar, J. E. (2008) Insulin-like growth factor (IGF) binding protein-4 is both a positive and negative regulator of IGF activity *in vivo*. *Mol. Endocrinol.* **22,** 1213–1225
16. Laursen, L. S., Kjaer-Sorensen, K., Andersen, M. H., and Oxvig, C. (2007) Regulation of insulin-like growth factor (IGF) bioactivity by sequential proteolytic cleavage of IGF binding protein-4 and -5. *Mol. Endocrinol.* **21,** 1246–1257
17. Conover, C. A., Bale, L. K., Overgaard, M. T., Johnstone, E. W., Laursen, U. H., Füchtbauer, E. M., Oxvig, C., and van Deursen, J. (2004) Metalloproteinase pregnancy-associated plasma protein A is a critical growth regulatory factor during fetal development. *Development* **131,** 1187–1194
18. DeChiara, T. M., Efstratiadis, A., and Robertson, E. J. (1990) A growth-deficiency phenotype in heterozygous mice carrying an insulin-like growth factor II gene disrupted by targeting. *Nature* **345,** 78–80
19. Bayes-Genis, A., Conover, C. A., Overgaard, M. T., Bailey, K. R., Christiansen, M., Holmes, D. R., Jr., Virmani, R., Oxvig, C., and Schwartz, R. S. (2001) Pregnancy-associated plasma protein A as a marker of acute coronary syndromes. *N. Engl. J. Med.* **345,** 1022–1029
20. Harrington, S. C., Simari, R. D., and Conover, C. A. (2007) Genetic deletion of pregnancy-associated plasma protein-A is associated with resistance to atherosclerotic lesion development in apolipoprotein E-deficient mice challenged with a high-fat diet. *Circ. Res.* **100,** 1696–1702
21. Mader, J. R., Resch, Z. T., McLean, G. R., Mikkelsen, J. H., Oxvig, C., Marler, R. J., and Conover, C. A. (2013) Mice deficient in PAPP-A show resistance to the development of diabetic nephropathy. *J. Endocrinol.* **219,** 51–58
22. Conover, C. A., Bale, L. K., Mader, J. R., Mason, M. A., Keenan, K. P., and Marler, R. J. (2010) Longevity and age-related pathology of mice deficient in pregnancy-associated plasma protein-A. *J. Gerontol. A Biol. Sci. Med. Sci.* **65,** 590–599
23. Junnila, R. K., List, E. O., Berryman, D. E., Murrey, J. W., and Kopchick, J. J. (2013) The GH/IGF-1 axis in ageing and longevity. *Nat. Rev. Endocrinol.* **9,** 366–376
24. Chang, A. C., Jellinek, D. A., and Reddel, R. R. (2003) Mammalian stanniocalcins and cancer. *Endocr. Relat. Cancer* **10,** 359–373
25. Gerritsen, M. E., and Wagner, G. F. (2005) Stanniocalcin: no longer just a fish tale. *Vitam. Horm.* **70,** 105–135
26. Yeung, B. H., Law, A. Y., and Wong, C. K. (2012) Evolution and roles of stanniocalcin. *Mol. Cell. Endocrinol.* **349,** 272–280
27. Gagliardi, A. D., Kuo, E. Y., Raulic, S., Wagner, G. F., and DiMattia, G. E. (2005) Human stanniocalcin-2 exhibits potent growth-suppressive properties in transgenic mice independently of growth hormone and IGFs. *Am. J. Physiol. Endocrinol. Metab.* **288,** E92–E105
28. Chang, A. C., Hook, J., Lemckert, F. A., McDonald, M. M., Nguyen, M. A., Hardeman, E. C., Little, D. G., Gunning, P. W., and Reddel, R. R. (2008) The murine stanniocalcin 2 gene is a negative regulator of postnatal growth. *Endocrinology* **149,** 2403–2410
29. Overgaard, M. T., Haaning, J., Boldt, H. B., Olsen, I. M., Laursen, L. S., Christiansen, M., Gleich, G. J., Sottrup-Jensen, L., Conover, C. A., and Oxvig, C. (2000) Expression of recombinant human pregnancy-associated plasma protein-A and identification of the proform of eosinophil major basic protein as its physiological inhibitor. *J. Biol. Chem.* **275,** 31128–31133
30. Søe, R., Overgaard, M. T., Thomsen, A. R., Laursen, L. S., Olsen, I. M., Sottrup-Jensen, L., Haaning, J., Giudice, L. C., Conover, C. A., and Oxvig, C. (2002) Expression of recombinant murine pregnancy-associated plasma protein-A (PAPP-A) and a novel variant (PAPP-Ai) with differential proteolytic activity. *Eur. J. Biochem.* **269,** 2247–2256
31. Niwa, H., Yamamura, K., and Miyazaki, J. (1991) Efficient selection for high-expression transfectants with a novel eukaryotic vector. *Gene.* **108,** 193–199
32. Mikkelsen, J. H., Resch, Z. T., Kalra, B., Savjani, G., Kumar, A., Conover, C. A., and Oxvig, C. (2014) Indirect targeting of IGF receptor signaling *in vivo* by substrate-selective inhibition of PAPP-A proteolytic activity. *Oncotarget* **5,** 1014–1025
33. Laursen, L. S., Chan, C. W., and ffrench-Constant, C. (2009) An integrin-contactin complex regulates CNS myelination by differential Fyn phosphorylation. *J. Neurosci.* **29,** 9174–9185
34. Gyrup, C., and Oxvig, C. (2007) Quantitative analysis of insulin-like growth factor-modulated proteolysis of insulin-like growth factor binding protein-4 and -5 by pregnancy-associated plasma protein-A. *Biochemistry* **46,** 1972–1980
35. Oxvig, C., Sand, O., Kristensen, T., Kristensen, L., and Sottrup-Jensen, L. (1994) Isolation and characterization of circulating complex between human pregnancy-associated plasma protein-A and proform of eosinophil major basic protein. *Biochim. Biophys. Acta* **1201,** 415–423
36. Mikkelsen, J. H., Steffensen, L. B., and Oxvig, C. (2014) Development of a recombinant antibody towards PAPP-A for immunohistochemical use in multiple animal species. *J. Immunol. Methods* **404,** 33–40
37. Greenfield, N. J. (2006) Using circular dichroism spectra to estimate protein secondary structure. *Nat. Protoc.* **1,** 2876–2890
38. Trindade, D. M., Silva, J. C., Navarro, M. S., Torriani, I. C., and Kobarg, J. (2009) Low-resolution structural studies of human stanniocalcin-1. *BMC Struct. Biol.* **9,** 57
39. Qin, X., Wergedal, J. E., Rehage, M., Tran, K., Newton, J., Lam, P., Baylink, D. J., and Mohan, S. (2006) Pregnancy-associated plasma protein-A increases osteoblast proliferation *in vitro* and bone formation *in vivo*. *Endocrinology* **147,** 5653–5661
40. Rehage, M., Mohan, S., Wergedal, J. E., Bonafede, B., Tran, K., Hou, D., Phang, D., Kumar, A., and Qin, X. (2007) Transgenic overexpression of pregnancy-associated plasma protein-A increases the somatic growth and skeletal muscle mass in mice. *Endocrinology* **148,** 6176–6185
41. Smith, G. C., Stenhouse, E. J., Crossley, J. A., Aitken, D. A., Cameron, A. D., and Connor, J. M. (2002) Early-pregnancy origins of low birth weight. *Nature* **417,** 916
42. Sjögren, K., Liu, J. L., Blad, K., Skrtic, S., Vidal, O., Wallenius, V., LeRoith, D., Törnell, J., Isaksson, O. G., Jansson, J. O., and Ohlsson, C. (1999) Liver-derived insulin-like growth factor I (IGF-I) is the principal source of IGF-I

in blood but is not required for postnatal body growth in mice. *Proc. Natl. Acad. Sci. U.S.A.* **96,** 7088–7092
43. Yakar, S., Liu, J. L., Stannard, B., Butler, A., Accili, D., Sauer, B., and LeRoith, D. (1999) Normal growth and development in the absence of hepatic insulin-like growth factor I. *Proc. Natl. Acad. Sci. U.S.A.* **96,** 7324–7329
44. Lango Allen, H., Estrada, K., Lettre, G., Berndt, S. I., Weedon, M. N., Rivadeneira, F., Willer, C. J., Jackson, A. U., Vedantam, S., Raychaudhuri, S., Ferreira, T., Wood, A. R., Weyant, R. J., Segrè, A. V., Speliotes, E. K., *et al.* (2010) Hundreds of variants clustered in genomic loci and biological pathways affect human height. *Nature* **467,** 832–838
45. Schoenebeck, J. J., and Ostrander, E. A. (2014) Insights into morphology and disease from the dog genome project. *Annu. Rev. Cell Dev. Biol.* **30,** 535–560
46. Rimbault, M., Beale, H. C., Schoenebeck, J. J., Hoopes, B. C., Allen, J. J., Kilroy-Glynn, P., Wayne, R. K., Sutter, N. B., and Ostrander, E. A. (2013) Derived variants at six genes explain nearly half of size reduction in dog breeds. *Genome Res.* **23,** 1985–1995
47. Olsen, H. S., Cepeda, M. A., Zhang, Q. Q., Rosen, C. A., Vozzolo, B. L., and Wagner, G. F. (1996) Human stanniocalcin: a possible hormonal regulator of mineral metabolism. *Proc. Natl. Acad. Sci. U.S.A.* **93,** 1792–1796
48. Chang, A. C., and Reddel, R. R. (1998) Identification of a second stanniocalcin cDNA in mouse and human: stanniocalcin 2. *Mol. Cell. Endocrinol.* **141,** 95–99
49. Varghese, R., Gagliardi, A. D., Bialek, P. E., Yee, S. P., Wagner, G. F., and Dimattia, G. E. (2002) Overexpression of human stanniocalcin affects growth and reproduction in transgenic mice. *Endocrinology* **143,** 868–876
50. Chang, A. C., Cha, J., Koentgen, F., and Reddel, R. R. (2005) The murine stanniocalcin 1 gene is not essential for growth and development. *Mol. Cell. Biol.* **25,** 10604–10610
51. Overgaard, M. T., Boldt, H. B., Laursen, L. S., Sottrup-Jensen, L., Conover, C. A., and Oxvig, C. (2001) Pregnancy-associated plasma protein-A2 (PAPP-A2), a novel insulin-like growth factor-binding protein-5 proteinase. *J. Biol. Chem.* **276,** 21849–21853
52. Conover, C. A., Boldt, H. B., Bale, L. K., Clifton, K. B., Grell, J. A., Mader, J. R., Mason, E. J., and Powell, D. R. (2011) Pregnancy-associated plasma protein-A2 (PAPP-A2): tissue expression and biological consequences of gene knockout in mice. *Endocrinology* **152,** 2837–2844
53. Pollak, M. (2012) The insulin and insulin-like growth factor receptor family in neoplasia: an update. *Nat. Rev. Cancer* **12,** 159–169
54. Welcsh, P. L., Lee, M. K., Gonzalez-Hernandez, R. M., Black, D. J., Mahadevappa, M., Swisher, E. M., Warrington, J. A., and King, M. C. (2002) BRCA1 transcriptionally regulates genes involved in breast tumorigenesis. *Proc. Natl. Acad. Sci. U.S.A.* **99,** 7560–7565
55. Joensuu, K., Heikkilä, P., and Andersson, L. C. (2008) Tumor dormancy: elevated expression of stanniocalcins in late relapsing breast cancer. *Cancer Lett.* **265,** 76–83